Published in final edited form as:
*JACC Cardiovasc Imaging*. 2012 February ; 5(2): 214–226. doi:10.1016/j.jcmg.2011.11.009.

# Targeted Metabolic Imaging to Improve the Management of Heart Disease

**Moritz Osterholt**[1], **Shiraj Sen**[1], **Vasken Dilsizian, MD**[2], and **Heinrich Taegtmeyer, MD, DPhil**[1]

[1]The University of Texas Medical School at Houston, Department of Internal Medicine/Division of Cardiology

[2]University of Maryland School of Medicine, Department of Diagnostic Radiology and Nuclear Medicine

## Abstract

Tracer techniques are powerful methods for assessing rates of biological processes in vivo. A case in point is intermediary metabolism of energy providing substrates, a central feature of every living cell. In the heart, the tight coupling between metabolism and contractile function offers an opportunity for the simultaneous assessment of cardiac performance at different levels in vivo: Coronary flow, myocardial perfusion, oxygen delivery, metabolism, and contraction. Non-invasive imaging techniques used to identify the metabolic footprints of either normal or perturbed cardiac function are discussed.

In order to contract under constantly changing environmental conditions, the healthy heart derives its energy from a variety of oxidizable organic compounds (1). When myocardial energy demands are increased acutely, the heart maintains the balance between its energetic supply and demand by shifting fluxes through existing metabolic pathways (2,3). Sustained increases in myocardial energy demand result in metabolic adaptations at a transcriptional level through selective upregulation of the synthesis and degradation of the enzymes that collectively make up metabolic pathways (4). In short, a striking system of checks and balances regulates contractile function in the heart and metabolism is at the center of the whole system.

Since the 1980s, the study of cardiac metabolism in the laboratory has been leveraged by clinicians using non-invasive imaging to distinguish heart muscle that is reversibly dysfunctional (viable myocardium) from muscle that is irreversibly dysfunctional (scar tissue) (5). The assessment of regional myocardial metabolism was first appreciated as a tool to guide therapeutic decisions for revascularization in patients with chronic ischemic left-ventricular dysfunction. Here the premise was that restoration of blood flow to viable ischemic tissue will result in restoration of oxidative metabolism and, as a consequence, normal contractile function. Similar imaging techniques are now explored to identify prospectively patients with reversible left ventricular dysfunction in order to improve both, quality of life and outcome (6,7).



Address for correspondence: Heinrich Taegtmeyer, MD, DPhil, University of Texas Medical School at Houston, Department of Internal Medicine, Division of Cardiology, 6431 Fannin, MSB 1.246, Houston, TX 77030, Phone: 713-500-6569, Fax: 713-500-0637, Heinrich.Taegtmeyer@uth.tmc.edu.

## REGULATION OF METABOLISM IN NORMAL AND FAILING HEART

The uptake of oxidizable fuel is tightly matched to the contractile work performed by the heart(8). Because oxygen extraction by the heart is nearly complete, increased rates of oxygen consumption can only be met by an increase in coronary flow (9). The normal heart oxidizes fat in preference to carbohydrates (the Randle hypothesis) (10), but it increases carbohydrate oxidation when stressed (11). When myocardial blood flow is impaired, the balance between cellular metabolism and contractile function is perturbed. The decrease in coronary flow and concomitant reduction in oxygen delivery triggers specific and coordinated responses in gene expression, including activation of HIF1α (12) and the reactivation of the fetal gene program (13), both of which improve the cardiomyocytes' tolerance to ischemia. Collectively, these changes represent the heart's adaptive processes resulting in cell survival, a phenomenon that we termed "programmed cell survival" some time ago (14,15). The term programmed cell survival contrasts programmed cell death or apoptosis, which occurs in the maladapted, failing heart. The metabolic derangements in the failing heart have been reviewed earlier (16,17). We have proposed that the non-ischemic, failing heart is drowning in fuel (18), and there is considerable metabolic heterogeneity in the failing human heart. Both are areas of active research and beyond the scope of this review.

Beyond supporting the metabolism of energy providing substrates, proteins that regulate metabolic pathways in the heart turn over themselves, as do sarcomeric proteins, cytoskeletal proteins, and other cellular components that are necessary for cardiac maintenance and growth. When subjected to stress, the heart undergoes hypertrophy, a process that demands increased energy supply. A large amount of this energy is likely required to fuel protein synthesis and protein quality control (19), suggesting the need for the cardiomyocyte to continually renew itself from within during times of growth. While regression of left ventricular hypertrophy has been associated with improved contractile function, its effects on myocardial energetics have yet to be characterized with non-invasive metabolic imaging.

## WHICH TRACERS FOR WHICH PATHWAYS?

Nuclear metabolic imaging uses targeted radiotracers to assess flux through specific metabolic pathways (by quantifying either the flux of energy-providing substrates or the steady-state metabolites). It is convenient to follow energy transfer in the heart muscle cell from the circulation (substrate and O2 delivery) to the cross-bridges (energy utilization) through a series of moiety conserved cycles (Figure 1). Specific radiotracers are available to assess perfusion, substrate uptake and delivery, as well as Krebs cycle turnover (oxygen consumption). We have represented the family of radiolabeled tracers by red arrows. In addition, we have highlighted the metabolic imaging modalities by magnetic resonance spectroscopy with either stable isotopes (e.g., $^{13}C$) or $^{31}P$ in the blue circles. Calcium ($Ca^{2+}$) is not an imaging agent but the ion has been included because it is the signal that links contraction and mitochondrial respiration (20). Radiotracer retention and/or metabolism is assessed by noninvasive techniques, such as single-photon emission computed tomography (SPECT) and positron emission tomography (PET).

Two classes of radiotracers are currently used to trace metabolic activity: labeled substrates or substrate analogs. Labeled substrates are taken up by heart muscle and either rapidly cleared or retained, while substrate analogs are taken up and retained only (Figure 2). Both will be discussed below in the context of their usefulness.

To assess *fatty acid utilization*, earlier studies used the labeled substrate $^{11}C$-palmitate. After its uptake into the cell and activation by binding to coenzyme A, $^{11}C$-palmitate undergoes

beta-oxidation, ultimately leading to the release of $^{11}CO2$. However, this technique requires a PET camera and an on-site cyclotron. As SPECT cameras were already available to the majority of nuclear cardiologists, the focus turned on the development of SPECT tracers for fatty acid oxidation. One of them is [$^{123}$I]-β-methyl-*p*-iodophenyl-pentadecanoic acid ($^{123}$I-BMIPP), a substrate analog that is rapidly taken up into the cardiomyocytes and which shows prolonged retention due to limited catabolism.

The current gold standard for evaluating *glucose metabolism* is 2-deoxy-2-($^{18}$F) fluoro-D-glucose ($^{18}$F-FDG) PET. $^{18}$F-FDG is a glucose analog that competes with glucose for phosphorylation by hexokinase. Once phosphorylated, it is trapped inside the cell and can neither be further metabolized, nor exported back out of the cell. We have demonstrated the retention of $^{18}$F-FDG in the isolated perfused heart at a constant, intermediate workload before (21) (Figure 3). Hearts were perfused with a buffer containing $^{18}$F-FDG for 60 minutes. During this time, radioactivity in the heart increased in a linear fashion. Note the retention of the tracer by the heart when the perfusate was switched to a tracer-free perfusate at 60 minutes (**arrow**). The drop in tissue radioactivity was caused by the wash-out of tracer from the ventricles, vascular and extracellular space. Also note that tracer uptake was linear with time by Patlak analysis (**insert**).

While the imaging of glucose and fatty acid metabolism in the heart has been well established in the past, imaging of *amino acid metabolism* has received less attention. In comparison to fatty acids and carbohydrates, amino acids are a more heterogeneous group of small organic compounds. The function of amino acids as building blocks for proteins and the intermediary metabolism of amino acids in the body was first investigated with stable isotopes by Schoenheimer in 1942 (22). The carbon skeleton of amino acids may enter the citric acid cycle and replenish the pool of its intermediates by a process termed anaplerosis, or be used for anaerobic energy provision (23). In 1954, Bing *et al.* reported that amino acids were extracted from the coronary blood and suggested that “a considerable fraction of the oxygen consumption of the heart can be ascribed to the breakdown of amino acids” (24). The intermediary metabolism of amino acids is complex. However, under aerobic conditions many amino acids, including the branched chain amino acids (BCAAs) leucine, isoleucine, and valine, are oxidized in the Krebs cycle (Figure 1). The BCAAs are essential amino acids with multiple roles in energy balance, nutrient signaling and protein homeostasis(25). The rate-limiting step in their catabolism is the α-ketoacid dehydrogenase reaction, an enzyme regulated by phosphorylation and dephosphorylation (26). Huang et al. has recently reviewed the role of defects in BCAA metabolism in heart disease (27). In spite of the physiologic importance of BCAA metabolism (and myocardial protein turnover in general), as yet no metabolic imaging strategies have been applied in the heart.

In contrast, amino acid metabolism in the ischemic heart has been investigated with $^{11}$C-glutamate. The rationale for this tracer is given by the anaerobic metabolism of glutamate to both alanine (28) and succinate (23). At the same time, we observed enhanced extraction of glutamate and enhanced release of alanine by hearts of patients with coronary artery disease (29). We suggested that this pattern was part of an adaptive process, where pyruvate is converted into alanine by the transfer of an amino group from glutamate, thereby reducing the formation of lactate out of pyruvate, which would ultimately inhibit glycolysis and thus anaerobic ATP production. Although the potential of using labeled amino acids for cardiac PET imaging was recognized 30 years ago (30), only a few investigators have used this technique to trace the footprints of myocardial ischemia. Several studies have assessed the uptake of $^{13}$N-glutamate in the ischemic heart, reporting either increased (31,32) or unchanged rates of uptake (33), relative to blood flow tracers as $^{13}$N-ammonia or $^{201}$Thallium ($^{201}$Tl). More recent studies used $^{11}$C-methionine for PET analysis of cardiac tissue after myocardial infarction (MI) (34). The investigators reported increased uptake

of $^{11}$C-methionine in infarcted areas during the acute phase after MI, while $^{201}$Tl and $^{18}$F-FDG uptake were reduced. Thus, the assessment of $^{11}$C-methionine uptake can be useful in monitoring the remodeling of the heart after MI. With the current notion that changes in amino acid metabolism are an “under-appreciated culprit” of heart disease, rather than just an epiphenomenon (27), studies addressing and validating the imaging of cardiac amino acid metabolism by using labeled amino acids are needed more than ever.

## METABOLIC REMODELING IN MYOCARDIAL ISCHEMIA

The heart protects itself from insufficient oxygen supply by downregulating mitochondrial oxidative metabolism. Moderate ischemia (75% reduction in coronary flow) shifts myocardial energy metabolism to an anaerobic state (35). During severe ischemia (90% reduction in coronary flow), myocardial glucose extraction increases while glucose uptake remains the same (36), at least until the degree of ischemia becomes so severe that substrate delivery and glycolysis are both inhibited by the accumulation of lactate (37). During prolonged severe ischemia, the decline of glucose uptake may be attenuated by various interventions protecting the heart against ischemic injury, such as an increase in the extracellular glucose concentration or the addition of insulin (38). Moreover, transcript levels of glucose transporters are also increased (39–41). In the absence of adaptive changes in metabolism, the resultant energy deficit ultimately leads to cell death, either by apoptosis or necrosis (14). Hence, acute and chronic metabolic adaptation to a temporary or sustained reduction in coronary blood flow conserves energy to protect the structural and functional integrity of the myocardium. Reversible metabolic changes, as a feature of sustained myocardial viability, will occur in the setting of diminished but not absent regional myocardial blood flow.

## ASSESSMENT OF MYOCARDIAL VIABILITY

To date, much has already been written about the assessment of myocardial viability (42). The principle is clear. Any transformational change in response to an altered environment requires a living or “viable” tissue. Let us consider the following: As already outlined above, the oxygen-deprived heart exhibits drastic changes in its metabolism leading to the development of left-ventricular dysfunction. Assessment of myocardial viability is needed in a situation, when left-ventricular dysfunction can either be permanent (due to myocardial cell death and formation of scar tissue) or reversible (in hibernating myocardium, which is ischemic but still viable). The benefit of revascularization for patients with coronary artery disease, for example, is known to be increasing with increasing amounts of hibernating myocardium (43). Metabolic imaging techniques as $^{18}$F-FDG PET can identify the extent of hibernating myocardium and therefore help to assess the benefit of revascularization in these patients (44).

By definition, hibernating myocardium shows chronic contractile dysfunction in the setting of reduced coronary flow reserve. After revascularization, myocardial function is restored, paralleled by an increase in coronary flow reserve (45). Hibernating myocardium can be assessed non-invasively with a variety of radiolabeled markers using different techniques. While SPECT tracers as $^{201}$Thallium chloride and $^{99m}$Technetium ($^{99m}$Tc)-labeled perfusion tracers (e.g., $^{99m}$Tc-tetrofosmin and $^{99m}$Tc-sestamibi) are primarily used as blood flow tracers, the uptake and retention of these agents inside the cell still requires intact cell membranes and viable cells. Hence, thallium and $^{99m}$Tc-labeled perfusion tracers can be used for viability assessment as well. These flow tracers when administered under resting conditions delineate presence or absence of scar tissue and its amount. As such, the information obtained with these flow tracers is analogous to that available through late contrast enhanced magnetic resonance imaging where the amount of residual non-enhancing

myocardium (or scar tissue) contains similar to the perfusion defect severity predictive information on the potential for functional recovery (46). However, beyond identifying regional blood flow, thallium differs from other flow tracers as being a monovalent cation with biologic properties that are similar to potassium. Like potassium, thallium is transported across the myocellular membrane via the sodium-potassium adenosine triphosphatase transport system. While the initial extraction and distribution of thallium in the myocardium are primarily a function of blood flow, the late redistribution phase of thallium is a function of regional myocardial potassium space (as the radiotracer has equilibrated between blood and myocytes). Thus, differences in thallium distributions between the early (myocardial perfusion phase) and delayed images reflect hypoperfused but viable (in the true sense of the term) myocardium. At the same time, although myocardium can be severely hypo-perfused, regional increase in glucose extraction via glucose transporter protein type 1 (GLUT1) results in up-regulated glucose uptake (termed a mismatch pattern) (Figure 4). This mismatch pattern is an indicator for hibernating myocardium, which can be salvaged by the restoration of blood flow. Therefore, metabolic imaging of myocardial viability may assist the early identification of patients who would benefit from revascularization therapies. This would decrease the risk/benefit ratio of revascularization and improve the patient's outcome and prognosis.

## IMAGING CARDIAC METABOLISM TO DETECT ANTECEDENT ISCHEMIA

The detection of even subtle metabolic alterations in the ischemic myocardium by metabolic imaging was first shown in a canine model of partial coronary artery occlusion and rapid atrial pacing (47). In subsequent occlusion-reperfusion studies, prolonged metabolic alterations were observed after 30 minutes of occlusion. These metabolic changes persisted for several weeks thereafter (48–51). The studies served as the experimental basis of subsequent clinical studies in which persistent reductions in fatty acid metabolism could be detected long after the resolution of the perfusion abnormality and ischemia (52–58). Thus, the application of a metabolic radiotracer for imaging, as opposed to a perfusion tracer, potentially extends the scope for noninvasive imaging of an ischemic event beyond the resolution of symptoms and allows monitoring long-term effects. The concept applies to tracers or tracer analogs of both, long-chain fatty acids and glucose. Their uptake by previously ischemic heart muscle is either decreased (in the case of fatty acids) or increased (in the case of glucose).

An exciting development in this field is the use of $^{123}$I-BMIPP to assess fatty acid metabolism with SPECT. In an open label Phase 2A clinical trial, patients with exercise-induced ischemia on a clinically indicated thallium SPECT study underwent rest $^{123}$I-BMIPP SPECT imaging within 30 hours of the exercise treadmill study (52). $^{123}$I-BMIPP was able to detect antecedent ischemic abnormality (with 91% agreement between $^{123}$I-BMIPP uptake and retention under resting conditions and $^{201}$Tl imaging under stress conditions). These findings were complemented by studies that interrogated the benefits of assessing altered glucose metabolism in patients undergoing exercise treadmill testing using $^{18}$F-FDG (53,54). A metabolic switch from predominant fatty acid use to predominant glucose use seems pivotal in preserving myocardial viability and likely represents the earliest adaptive response to myocardial ischemia (53). Applying a dual-isotope $^{99m}$Tc-sestambi and $^{18}$F-FDG simultaneous-injection-and acquisition protocol, investigators have shown that a metabolic switch from fatty acid to glucose use occurs promptly when myocardial ischemia is induced during exercise. Moreover, the exercise-induced metabolic switch to glucose may persist for 24 hours, despite restoration of blood flow at rest (54) (55). Together, these reports with fatty acid and glucose analogues suggest an interdependence of the increased glucose uptake and the diminished fatty acid uptake. Whether there are temporal differences between the two processes cannot be addressed

conclusively, because the two radiotracers ($^{123}$I-BMIPP and $^{18}$F-FDG) were not injected at the same time and in the same patient.

In a recent multicenter clinical trial, patients presenting to the emergency department with suspected acute coronary syndrome were imaged with $^{123}$I-BMIPP within 30 hours of symptom cessation (56). The initial clinical diagnosis was based on symptoms, electrocardiographic changes, and elevated serum troponin levels, while the final diagnosis was based on all available data (including coronary angiography and stress SPECT) but not $^{123}$I-BMIPP SPECT. Final diagnoses were adjudicated by a blinded committee into "positive for acute coronary syndrome", "intermediate likelihood of acute coronary syndrome" or "negative for acute coronary syndrome". Compared to the clinical impression alone, the combination of $^{123}$I-BMIPP with the initial clinical diagnosis increased sensitivity for identifying patients with acute coronary syndrome, negative predictive value, and positive predictive value, with the same specificity. The findings suggest that the addition of $^{123}$I-BMIPP imaging data to the clinical impression provides incremental value toward the early diagnosis of acute coronary syndrome in the emergency department. These results are consistent with earlier findings in patients with acute chest pain who underwent coronary angiography, in which the sensitivity of $^{123}$I-BMIPP for detecting an obstructive coronary artery disease or provocable spasm was 74%, when $^{123}$I-BMIPP imaging was carried out within 3 days of presenting symptoms (57). Delayed recovery of fatty acid metabolism as assessed by SPECT for up to 30 hours after the resolution of transient myocardial ischemia, provides the potential for diagnosing antecedent myocardial ischemia, a phenomenon that we have termed "ischemic memory" or "metabolic stunning" (58).

## METABOLIC REMODELING OF THE HEART IN DIABETES AND OBESITY

Non-invasive imaging also provides distinct advantages to studying the effects of systemic metabolic diseases, such as diabetes and obesity, on the heart. The introduction of new animal models of insulin resistance and type 2 diabetes has resulted in a deeper understanding of the biochemical derangements underlying metabolic and structural remodeling of the myocardium. We have proposed that metabolic remodeling precedes, triggers, and maintains functional and structural remodeling, all of which can be traced by noninvasive imaging techniques (2). With diabetes and obesity, fatty acid delivery to the heart is increased. In combination with increased incorporation of fatty acid translocase into the plasma membrane (59), excess fatty acid supply results in increased intracellular levels of fatty acids. After being activated to acyl-CoA, fatty acids can serve many purposes, including energy production (via mitochondrial β-oxidation), posttranslational protein modification, or triglyceride synthesis (60). However, cardiomyocytes have only a limited capacity to store triglycerides and an increase in triglyceride levels in the heart can be used as an indicator of a deleterious imbalance between fatty acid uptake and oxidation (61) that eventually culminates in lipotoxicity. Indeed, myocardial lipid overload induces a lipotoxic cardiomyopathy even in the absence of systemic perturbations in fatty acid metabolism (62).

In patients with impaired glucose tolerance, myocardial steatosis was found using $^{1}$H magnetic resonance spectroscopy and shown to precede the onset of type 2 diabetes and cardiac dysfunction (63). While increased intracellular triglyceride levels are considered more as a marker rather than a mediator of lipotoxicity (64), increased levels of acyl-CoA have several detrimental effects: 1) Beside triglycerides, levels of diacylglycerol (DAG) are enhanced, which has been implicated in the activation of protein kinase C theta (PKCθ). Chronic activation of PKCθ impairs insulin signaling by phosphorylating IRS-1 on serine residues (65,66); 2) concentration of ceramide, potentially cardiotoxic due to its role in apoptotic signaling, is increased, which is associated with the development of cardiomyopathies in diabetes and obesity (67); 3) excess fatty acids and their oxidation are

associated with increased production of reactive oxygen species that are known to compromise a variety of other cellular processes and to induce adverse cardiac remodeling (68). However, a recent study raises doubt about the role of DAG and ceramide as mediators of lipotoxic heart disease. Son *et al.* assessed metabolic changes in a PPARα-deficient model of PPARγ-induced cardiolipotoxicity and reported increased rates of fatty acid oxidation with preserved cardiac function and improved survival despite no changes in triglycerides, DAG and ceramide levels (69). This now questions the biological relevance of these lipotoxic intermediates in mediating contractile dysfunction.

## METABOLIC REMODELING IN THE HEART OF PATIENTS WITH PRE-CLINICAL AND END-STAGE RENAL DISEASE

While myocardial infarction and ischemic heart disease account for the significant portion of patients with heart failure and left ventricular remodeling, several sequelae of renal failure can also contribute to left ventricular metabolic remodeling, termed uremic cardiomyopathy (70–72) (Figure 5). Kidney disease affects over 19 million American adults, and the prevalence of moderate-to-severe chronic kidney disease (CKD) in individuals who are not on dialysis is high (73). The United States Renal Data System has reported near-equivalent rates of myocardial infarction and cardiac death in dialysis patients and an approximately 10-fold higher rate of heart failure in the same population (74). The common occurrence of heart failure in the dialysis population is thought to be related to left ventricular hypertrophy that occurs frequently in patients with CKD. Hypertension is common among patients with renal disease and has been suggested to be volume-dependent. Therefore, both volume- and pressure-overload would trigger left-ventricular hypertrophy, while further changes in structure (e.g., anterior wall thickening and arterial stiffening) and hormone status (i.e., activation of neurohormones) take place. Concomitantly, renal function declines and CKD progresses.

The so-called uremic cardiomyopathy probably has multiple causes. One of them involves a myocyte-capillary mismatch, with a diminished vascular supply relative to the number and volume of functioning myocytes (75). As in the ischemic heart, the oxygen-poor milieu leads to a decline in aerobic myocardial fatty acid utilization and a shift to anaerobic glycolytic metabolism, with increased uptake of glucose as the principal energy providing substrate (76,77). The shift from a predominance of aerobic (fatty acid) to anaerobic (glucose) metabolism appears to account for a significant portion of the excessive cardiovascular morbidity and mortality observed across all stages of kidney disease (70,78). Thus, the application of a non-invasive, quantitative PET technique to monitor myocardial metabolism in early-stage early stage kidney disease has potential to identify deleterious changes in cardiac metabolism prior to its manifestation as contractile dysfunction and cardiac hypertrophy.

### Pre-Clinical Myocardial Metabolic Alterations in Chronic Kidney Disease

$^{18}$F-FDG PET images are usually interpreted qualitatively in areas with myocardial perfusion deficits at rest and designated as either metabolism-perfusion mismatch (indicating viable myocardium) or match (indicating scarred myocardium) defects. However, detection of early, pre-clinical myocardial metabolic alterations can be limited with qualitative assessment of regional $^{18}$F-FDG uptake. Although the distribution of $^{18}$F-FDG uptake may visually appear homogeneous throughout the left ventricular myocardium, absolute myocardial glucose utilization may be abnormal. Quantitative assessment with PET may identify alterations in whole myocardial glucose uptake (MGU) before clinical, functional, and prognostic consequences ensue.

The feasibility of employing quantitative MGU with PET to gain additional insight into the alterations of myocardial metabolism in CKD patients was recently studied (77). The authors demonstrated a significant inverse correlation between myocardial glucose uptake and renal function, assessed by estimated glomerular filtration rate (eGFR), in CKD patients. The relationship between MGU and eGFR could not be ascribed to demographic factors or cardiac workload. Thus, $^{18}$F-FDG PET may be an effective tool to investigate pre-clinical changes in myocardial metabolism in CKD.

### Myocardial Metabolic Alterations in End-Stage Chronic Kidney Disease

In hemodialysis patients without coronary artery disease, investigators have demonstrated alterations in myocardial fatty acid utilization in subsets of patients by using $^{123}$I-BMIPP SPECT. Reduced uptake of $^{123}$I-BMIPP correlates with reduced left ventricular ejection fraction and increased systemic insulin resistance (76). While some studies have demonstrated that systemic insulin resistance is associated with heart failure and cardiac insulin resistance (79) others have argued that it does not (80). The importance of assessing metabolic changes in the heart of patients with end-stage CKD was, however, underlined by another study where impaired $^{123}$I-BMIPP uptake was shown to identify patients with a high risk for cardiac death (78). The application of metabolic imaging with PET and SPECT tracers has the potential to offer useful insights into the pathogenesis for uremic cardiomyopathy and to point towards therapies for this disease. For example, carnitine deficiency is known to be common in end-stage renal disease and supplementation to patients on dialysis has been evaluated as a potential treatment for heart failure and hypotension (81). At least one study has used SPECT to examine the effect of carnitine supplementation on free fatty acid metabolism in patients with end-stage renal disease (82). The study demonstrated enhanced washout of myocardial 123I-BMIPP with carnitine treatment but no change in the heart-to-mediastinal ratio. The relatively preserved heart-to-mediastinal $^{123}$I-BMIPP uptake in the chronic hemodialysis patients suggests that the myocardial ATP content in these patients (hence ATP-dependent conversion of $^{123}$I-BMIPP to $^{123}$I-BMIPP-CoA) had not decreased in these patients despite carnitine deficiency. As such, there was no accelerated back diffusion of the non-metabolized radiotracer. However, because carnitine is essential for the transport of long-chain fatty acids from the cytoplasm into the matrix of mitochondria (the site of γ-oxidation), decreased carnitine availability results in longer residence of free fatty acids in the cytoplasm (in the form of $^{123}$I-BMIPP-CoA), as reflected by the lower washout rate of the radiotracer before carnitine administration. These findings are supported by the experimental observation in rats exhibiting prolonged retention of $^{123}$I-BMIPP in the myocardium when pretreated with a mitochondrial carnitine acyltransferase I inhibitor (83).

## NEW HORIZONS

### METABOLOMICS

Our current knowledge of the dynamics of intermediary metabolism remains fragmented and poorly integrated into the biology of the cell. The new and powerful tools of systems biology give a fresh approach to the diagnosis and treatment of different forms of heart disease. A case in point is the field of metabolomics. In analogy to the genome, the transcriptome, and the proteome, the metabolome has been defined as the total set of low molecular weight metabolites. The techniques of metabolomics (in particular nuclear magnetic resonance and mass spectroscopy) allow us to analyze changes in the metabolome in a given system. A major advantage of this metabolic profiling is the comparatively small number of possible targets: The Human Metabolome Database currently lists approximately 7,900 small metabolites, compared to 25,000 genes, 100,000 transcripts, and 1,000,000 proteins (84). Further, metabolites may show a better correlation with a disease's phenotype

than mRNAs or proteins, as they are further proximal reporters of a pathological process. Recent studies have delivered promising results and reported new markers for the development of type 2 diabetes (85) or coronary artery disease and subsequent cardiovascular events (86)(96).

Considering our hypothesis of metabolic changes preceding and triggering structural and functional changes in the heart, metabolomics can be useful beyond the mere exploration of biomarkers and assist the search for mediators of cardiovascular diseases. However, the impact of changes in the metabolome is debated and additional mechanistic studies would be needed to define the biological relevance of such changes. Although the use of metabolomics for assessing cardiovascular diseases is still in its infancy, it may soon be a powerful tool in the quest for alterations in metabolite levels and determining their pathophysiological impact.

## TRACKING THE FATE OF TRANSPLANTED STEM CELLS

Myocardial regeneration through stem cell injection is a beguiling concept, which to date has produced mixed results. Laboratory experiments and clinical trials suggest that cell-based therapies can improve cardiac function (87). Several experimental strategies to “remuscularize” and revascularize the failing heart using adult stem cells or pluripotent stem cells, cellular reprogramming or tissue engineering are in progress and offer unique opportunities for metabolic imaging.

After MI, patients have a high risk of developing heart failure due to cardiomyocyte death. Although the current treatments of MI aim on reducing the extent of cell death in the heart, they cannot restore myocardial contractility. With a cell-based therapy, myocytes can be generated out of adult, autologously transplanted stem cells and therefore prevent the progression into heart failure. While the recent development in the field of stem cell therapy is out of the scope of this review, it is appropriate to comment on using imaging techniques to track transplanted stem cells in vivo. Although preclinical studies have delivered promising data, concerns about dose requirements, localization after injection as well as viability impede the clinical use of autologously transplanted stem cells. All of these aspects can be assessed with the help of non-invasive imaging techniques.

In general, stem cells can be tracked with different imaging methods such as MRI, PET, and SPECT. Further, multimodality approaches, combining PET or SPECT with MRI or CT, merge the advantages and data sets delivered by each imaging technique itself (88). Stem cells can be labeled with radioactive markers prior to transplantation to assess their localization in the host’s body. However, concerns about the dissociation of the radionuclide from the stem cell have questioned the reliability of this technique for long-time studies, although it is a valid method to determine the success of a transplantation directly after delivery (88). Nonetheless, metabolic imaging of stem cells with $^{18}$F-FDG has produced promising results tracking the homing of $CD34^{+}$ cells to infracted myocardium (Figure 6) (89). A different labeling technique uses reporter genes that are introduced into the stem cells or the host genome. Besides the ability to perform long-time studies, the use of reporter genes allows the investigator or clinician to assess stem cell survival, as only viable cell produce the reporter probe. A recent study by Lee *et al.* has demosntrated the applicability of these techniques in a large-animal model (90). Briefly, the investigators generated induced pluripotent stem cells (iPSCs) from adipose stromal cells in a canine model and transduced these iPSCs with a triple-fusion reporter gene that included the herpex simplex truncated thymidine kinase. After injection of 9-[4-[(18)F]fluoro-3-(hydroxymethyl)butyl]guanine ($^{18}$F-FHBG) they could determine the accumulation of iPSCs (as increased tracer activity) in the anterior wall and confirm its localization by MRI and co-labeling of iPSCs with iron oxide particles. Improving stem cell targeting and reparative

capacity will also rely heavily on metabolic imaging with PET in the future (91). While the usefulness of this strategy is beyond question, little work has been done in this area until now.

## CONCLUSIONS

In recent years, the tools of molecular and cellular biology have provided new insights into the complex mechanisms of metabolic pathways and the multitude of potential targets which can be explored for the treatment of various heart diseases. SPECT and PET imaging techniques provide a sensitive, non-invasive, quantitative tool for investigating pre-clinical and clinical abnormalities in myocardial perfusion, metabolism, enzymatic or receptor derangements and allow for monitoring disease progression and the effectiveness of medical therapy. The new fields of metabolomics and stem cell imaging offer challenges to both the experimental biologist and the clinical cardiologist to refine the tools of metabolic imaging for the diagnosis and treatment of myocardial diseases.

## ABBREVIATIONS

| | |
|---|---|
| **SPECT** | single-photon emission computed tomography |
| **PET** | positron emission tomography |
| **$^{123}$I-BMIPP** | [$^{123}$I]-β-methyl-*p*-iodophenyl-pentadecanoic acid |
| **$^{18}$F-FDG** | $^{18}$F-fluorodeoxyglucose |
| **$^{201}$T** | $^{201}$Thallium |
| **$^{99m}$Tc** | $^{99m}$Technetium |
| **DAG** | diacylglycerol |
| **CKD** | chronic kidney disease |
| **MGU** | myocardial glucose uptake |
| **(A)MI** | (acute) myocardial infarction |

## References


1. Taegtmeyer H, Hems R, Krebs HA. Utilization of energy-providing substrates in the isolated working rat heart. Biochem J. 1980; 186:701–11. [PubMed: 6994712]
2. Taegtmeyer H, Golfman L, Sharma S, Razeghi P, van Arsdall M. Linking gene expression to function: Metabolic flexibility in the normal and diseased heart. Ann N Y Acad Sci. 2004; 1015:202–13. [PubMed: 15201161]
3. Katz AM. Molecular biology in cardiology, a paradigmatic shift. J Mol Cell Cardiol. 1988; 20:355–66. [PubMed: 3050135]
4. Taegtmeyer, H. Fueling the heart: Multiple roles for cardiac metabolism. In: JT, W.; JN, C.; HJJ, W.; DR, H., editors. Cardiovascular Medicine. 3. London: Springer-Verlag (London) Ltd; 2007. p. 1157-75.
5. Tillisch J, Brunken R, Marshall R, et al. Reversibility of cardiac wall-motion abnormalities predicted by positron tomography. N Engl J Med. 1986; 314:884–8. [PubMed: 3485252]
6. Di Carli MF, Davidson M, Little R, et al. Value of metabolic imaging with positron emission tomography for evaluating prognosis in patients with coronary artery disease and left ventricular dysfunction. Am J Cardiol. 1994; 73:527–33. [PubMed: 8147295]
7. Di Carli M, Asgarzadie F, Schelbert HR, et al. Quantitative relation between myocardial viability and improvement in heart failure symptoms after revascularization in patients with ischemic cardiomyopathy. Circulation. 1995; 92:3436–44. [PubMed: 8521565]

8. Sorokina N, O'Donnell JM, McKinney RD, et al. Recruitment of compensatory pathways to sustain oxidative flux with reduced carnitine palmitoyltransferase i activity characterizes inefficiency in energy metabolism in hypertrophied hearts. Circulation. 2007; 115:2033–41. [PubMed: 17404155]
9. Katz, AM. Physiology of the Heart. 5. Philadelphia: Lippincott, Williams & Wilkins; 2011.
10. Randle PJ, Garland PB, Hales CN, Newsholme EA. The glucose fatty-acid cycle. Its role in insulin sensitivity and the metabolic disturbances of diabetes mellitus. Lancet. 1963; 1:785–9. [PubMed: 13990765]
11. Goodwin GW, Taylor CS, Taegtmeyer H. Regulation of energy metabolism of the heart during acute increase in heart work. J Biol Chem. 1998; 273:29530–9. [PubMed: 9792661]
12. Lee SH, Wolf PL, Escudero R, Deutsch R, Jamieson SW, Thistlethwaite PA. Early expression of angiogenesis factors in acute myocardial ischemia and infarction. N Engl J Med. 2000; 342:626–33. [PubMed: 10699162]
13. Depre C, Shipley GL, Chen W, et al. Unloaded heart in vivo replicates fetal gene expression of cardiac hypertrophy. Nat Med. 1998; 4:1269–75. [PubMed: 9809550]
14. Depre C, Taegtmeyer H. Metabolic aspects of programmed cell survival and cell death in the heart. Cardiovasc Res. 2000; 45:538–48. [PubMed: 10728375]
15. Taegtmeyer, H. Modulation of responses to myocardial ischemia: Metabolic features of myocardial stunning, hibernation and ischemic preconditioning. In: Dilsizian, V., editor. Myocardial Viability from Cellular Physiology to Clinical Decision Making. New York: Futura Publishing Co; 2000. p. 25-36.
16. Gropler RJ, Geltman EM, Sampathkumaran K, et al. Functional recovery after coronary revascularization for chronic coronary artery disease is dependent on maintenance of oxidative metabolism. J Am Coll Cardiol. 1992; 20:569–77. [PubMed: 1512335]
17. Herrero P, Staudenherz A, Walsh JF, Gropler RJ, Bergmann SR. Heterogeneity of myocardial perfusion provides the physiological basis of perfusable tissue index. J Nucl Med. 1995; 36:320–7. [PubMed: 7830138]
18. Taegtmeyer H. The failing heart. N Engl J Med. 2007; 356:2545–6. author reply 6. [PubMed: 17575596]
19. Lane N, Martin W. The energetics of genome complexity. Nature. 2010; 467:929–34. [PubMed: 20962839]
20. Maack C, O'Rourke B. Excitation-contraction coupling and mitochondrial energetics. Basic Res Cardiol. 2007; 102:369–92. [PubMed: 17657400]
21. Nguyen VT, Mossberg KA, Tewson TJ, et al. Temporal analysis of myocardial glucose metabolism by 2-[18f]fluoro-2-deoxy-d-glucose. Am J Physiol. 1990; 259:H1022–31. [PubMed: 2221110]
22. Schoenheimer, R. The dynamic state of body constituents. Cambridge, MA: Harvard University Press; 1942.
23. Taegtmeyer H. Metabolic responses to cardiac hypoxia: Increased production of succinate by rabbit papillary muscles. Circ Res. 1978; 43:808–15. [PubMed: 709743]
24. Bing RJ, Siegel A, Ungar I, Gilbert M. Metabolism of the human heart. II. Studies on fat, ketone and amino acid metabolism. Am J Med. 1954; 16:504–15. [PubMed: 13148192]
25. Krebs HA, Lund P. Aspects of the regulation of the metabolism of branched-chain amino acids. Adv Enzyme Regul. 1976; 15:375–94. [PubMed: 19935]
26. Lu G, Sun H, She P, et al. Protein phosphatase 2cm is a critical regulator of branched-chain amino acid catabolism in mice and cultured cells. J Clin Invest. 2009; 119:1678–87. [PubMed: 19411760]
27. Huang Y, Zhou M, Sun H, Wang Y. Branched-chain amino acid metabolism in heart disease: An epiphenomenon or a real culprit? Cardiovasc Res. 2011; 90:220–3. [PubMed: 21502372]
28. Taegtmeyer H, Peterson MB, Ragavan VV, Ferguson AG, Lesch M. *De novo* alanine synthesis in isolated oxygen-deprived rabbit myocardium. J Biol Chem. 1977; 252:5010–8. [PubMed: 17612]
29. Mudge GH Jr, Mills RM Jr, Taegtmeyer H, Gorlin R, Lesch M. Alterations of myocardial amino acid metabolism in chronic ischemic heart disease. J Clin Invest. 1976; 58:1185–92. [PubMed: 993339]

30. Henze E, Schelbert HR, Barrio JR, et al. Evaluation of myocardial metabolism, with n-13- and c-11-labeled amino acids and positron computed tomography. J Nucl Med. 1982; 23:671–81. [PubMed: 6980971]
31. Zimmermann R, Tillmans H, Knopp WH. Regional myocardial $^{13}$n-glutamate uptake in patients with coronary artery disease. J Am Coll Cardiol. 1988; 11:549–56. [PubMed: 3343457]
32. Knapp W, Helus F, Ostertag H, Tilmanns H, Kuebler W. Uptake and turnover of l-[$^{13}$n] glutamate in the normal human heart and patients with coronary artery disease. Eur J Nucl Med. 1982; 7:211–5. [PubMed: 6124422]
33. Krivokapich J, Barrio JR, Huang SC, Schelbert HR. Dynamic positron tomographic imaging with nitrogen-13 glutamate in patients with coronary artery disease: Comparison with nitrogen-13 ammonia and fluorine-18 fluorodeoxyglucose imaging. J Am Coll Cardiol. 1990; 16:1158–67. [PubMed: 1977778]
34. Morooka M, Kubota K, Kadowaki H, et al. 11c-methionine pet of acute myocardial infarction. J Nucl Med. 2009; 50:1283–7. [PubMed: 19617334]
35. Bolukoglu H, Goodwin GW, Guthrie PH, Carmical SG, Chen TM, Taegtmeyer H. Metabolic fate of glucose in reversible low-flow ischemia of the isolated working rat heart. Am J Physiol. 1996; 270:H817–26. [PubMed: 8780175]
36. Stanley W, Hall J, Stone C, Hacker T. Acute myocardial ischemia causes a transmural gradient in glucose extraction but not glucose uptake. Am J Physiol. 1992; 262:H91–H6. [PubMed: 1733326]
37. Neely JR, Grotyohann LW. Role of glycolytic products in damage to myocardium: Dissociation of adenosine triphosphate levels and recovery of function of reperfused canine myocardium. Circ Res. 1984; 55:816–24. [PubMed: 6499136]
38. Vanoverschelde JL, Janier MF, Bakke JE, Marshall DR, Bergmann SR. Rate of glycolysis during ischemia determines extent of ischemic injury and functional recovery after reperfusion. Am J Physiol. 1994; 267:H1785–H94. [PubMed: 7977809]
39. Shetty M, Loeb JN, Ismail-Beigi F. Enhancement of glucose transport in response to inhibition of oxidative metabolism: Pre- and post-translational mechanisms. Am J Physiol. 1992; 262:C527–C32. [PubMed: 1539639]
40. Bashan N, Burdett E, Guma A, et al. Mechanisms of adaptation of glucose transporters to changes in the oxidative chain of muscle and fat cells. Am J Physiol. 1993; 264:C430–C40. [PubMed: 8447373]
41. Shetty M, Ismail-Beigi N, Loeb JN, Ismail-Beigi F. Induction of GLUT1 mRNA in response to inhibition of oxidative phosphorylation. Am J Physiol. 1993; 265:C1224–C9. [PubMed: 7694490]
42. Dilsizian, V. Myocardial viability: A clinical and scientific treatise. Armonk, NY: Futura Publishing Company, Inc; 2000.
43. D'Egidio G, Nichol G, Williams KA, et al. Increasing benefit from revascularization is associated with increasing amounts of myocardial hibernation: A substudy of the PARR-2 Trial. JACC Cardiovasc Imaging. 2009; 2:1060–8. [PubMed: 19761983]
44. Chatterjee K. Is detection of hibernating myocardium necessary in deciding revascularization in systolic heart failure? Am J Cardiol. 2010; 106:236–42. [PubMed: 20599009]
45. Camici PG, Prasad SK, Rimoldi OE. Stunning, hibernation, and assessment of myocardial viability. Circulation. 2008; 117:103–14. [PubMed: 18172050]
46. Dilsizian V. Cardiac magnetic resonance versus SPECT: Are all noninfarct myocardial regions created equal? J Nucl Cardiol. 2007; 14:9–14. [PubMed: 17276300]
47. Schelbert HR, Henze E, Phelps ME, Kuhl DE. Assessment of regional myocardial ischemia by positron-emission computed tomography. Am Heart J. 1982; 103:588–97. [PubMed: 6978056]
48. Schwaiger M, Schelbert H, Ellison D, et al. Sustained regional abnormalities in cardiac metabolism after transient ischemia in the chronic dog model. J Am Coll Cardiol. 1985; 6:337–47.
49. Fujibayashi Y, Yonekura Y, Takemura Y, et al. Myocardial accumulation of iodinated beta-methyl-branched fatty acid analogue, iodine-125–15-(p-iodophenyl)-3-(r,s) methylpentadecanoic acid (BMIPP), in relation to ATP concentration. J Nucl Med. 1990; 31:1818–22. [PubMed: 2230994]

50. Hosokawa R, Nohara R, Fujibayashi Y, et al. Myocardial kinetics of iodine-123-BMIPP in canine myocardium after regional ischemia and reperfusion: Implications for clinical SPECT. J Nucl Med. 1997; 38:1857–63. [PubMed: 9430458]
51. Dormehl IC, Hugo N, Rossouw D, White A, Feinendegen LE. Planar myocardial imaging in the baboon model with iodine-123-15-(iodophenyl)pentadecanoic acid (ippa) and iodine-123-15-(p-iodophenyl)-3-r,s-methylpentadecanoic acid (BMIPP), using time-activity curves for evaluation of metabolism. Nucl Med Biol. 1995; 22:837–47. [PubMed: 8547881]
52. Dilsizian V, Bateman TM, Bergmann SR, et al. Metabolic imaging with beta-methyl-p-[(123)i]-iodophenyl-pentadecanoic acid identifies ischemic memory after demand ischemia. Circulation. 2005; 112:2169–74. [PubMed: 16186423]
53. He Z, Shi R, Wu Y, et al. Direct imaging of exercise induced myocardial ischemia with fluorine-18 labeled deoxyglucose and tc-99m-sestamibi in coronary artery disease. Circulation. 2003; 108:1208–13. [PubMed: 12939208]
54. Dou KF, Yang MF, Yang YJ, Jain D, He ZX. Myocardial $^{18}$F-FDG uptake after exercise-induced myocardial ischemia in patients with coronary artery disease. J Nucl Med. 2008; 49:1986–91. [PubMed: 18997035]
55. Dilsizian V. $^{18}$F-FDG uptake as a surrogate marker for antecedent ischemia. J Nucl Med. 2008; 49:1909–11. [PubMed: 18997055]
56. Kontos MC, Dilsizian V, Weiland F, et al. Iodofiltic acid i 123 (BMIPP) fatty acid imaging improves initial diagnosis in emergency department patients with suspected acute coronary syndromes: A multicenter trial. J Am Coll Cardiol. 2010; 56:290–9. [PubMed: 20633821]
57. Kawai Y, Tsukamoto E, Nozaki Y, Morita K, Sakurai M, Tamaki N. Significance of reduced uptake of iodinated fatty acid analogue for the evaluation of patients with acute chest pain. J Am Coll Cardiol. 2001; 38:1888–94. [PubMed: 11738290]
58. Taegtmeyer H, Dilsizian V. Imaging myocardial metabolism and ischemic memory. Nat Clin Pract Cardiovasc Med. 2008; 5 (Suppl 2):S42–8. [PubMed: 18641606]
59. Steinbusch LK, Schwenk RW, Ouwens DM, Diamant M, Glatz JF, Luiken JJ. Subcellular trafficking of the substrate transporters GLUT4 and CD36 in cardiomyocytes. Cell Mol Life Sci. 2011
60. Faergeman N, Knudsen J. Role of long-chain fatty acyl-coa esters in the regulation of metabolism and in cell signalling. Biochem J. 1997; 323:1–12. [PubMed: 9173866]
61. Zhang L, Keung W, Samokhvalov V, Wang W, Lopaschuk GD. Role of fatty acid uptake and fatty acid beta-oxidation in mediating insulin resistance in heart and skeletal muscle. Biochim Biophys Acta. 2010; 1801:1–22. [PubMed: 19782765]
62. Glenn DJ, Wang F, Nishimoto M, et al. A murine model of isolated cardiac steatosis leads to cardiomyopathy. Hypertension. 2011; 57:216–22. [PubMed: 21220706]
63. McGavock JM, Lingvay I, Zib I, et al. Cardiac steatosis in diabetes mellitus: A 1h-magnetic resonance spectroscopy study. Circulation. 2007; 116:1170–5. [PubMed: 17698735]
64. Brookheart RT, Michel CI, Schaffer JE. As a matter of fat. Cell Metab. 2009; 10:9–12. [PubMed: 19583949]
65. Griffin ME, Marcucci MJ, Cline GW, et al. Free fatty acid-induced insulin resistance is associated with activation of protein kinase c theta and alterations in the insulin signaling cascade. Diabetes. 1999; 48:1270–4. [PubMed: 10342815]
66. Itani SI, Pories WJ, Macdonald KG, Dohm GL. Increased protein kinase c theta in skeletal muscle of diabetic patients. Metabolism. 2001; 50:553–7. [PubMed: 11319716]
67. Park TS, Hu Y, Noh HL, et al. Ceramide is a cardiotoxin in lipotoxic cardiomyopathy. J Lipid Res. 2008; 49:2101–12. [PubMed: 18515784]
68. Dirkx E, Schwenk RW, Glatz JF, Luiken JJ, van Eys GJ. High fat diet induced diabetic cardiomyopathy. Prostaglandins Leukot Essent Fatty Acids. 2011; 85:219–25. [PubMed: 21571515]
69. Son NH, Yu S, Tuinei J, et al. Ppargamma-induced cardiolipotoxicity in mice is ameliorated by PPARalpha deficiency despite increases in fatty acid oxidation. J Clin Invest. 2010; 120:3443–54. [PubMed: 20852389]

70. Dilsizian V, Fink JC. Deleterious effect of altered myocardial fatty acid metabolism in kidney disease. J Am Coll Cardiol. 2008; 51:146–8. [PubMed: 18191739]
71. Raine AE. The heart and renal failure. Contrib Nephrol. 1994; 109:76–83. [PubMed: 7956233]
72. Raine AE, Seymour AM, Roberts AF, Radda GK, Ledingham JG. Impairment of cardiac function and energetics in experimental renal failure. J Clin Invest. 1993; 92:2934–40. [PubMed: 8254048]
73. Coresh J, Selvin E, Stevens LA, et al. Prevalence of chronic kidney disease in the United States. J Am Med Assn. 2007; 298:2038–47.
74. United States RDS. Diseases NIoDaDaK. USRDS 2006 Annual Data Report: Atlas of end-stage renal disease in the US. National Institutes of Health; 2006.
75. Tyralla K, Amanna K. Morphology of the heart and arteries in renal failure. Kidney Inst. 2003; 63:S80–S3.
76. Nishimura M, Murase M, Hashimoto T, et al. Insulin resistance and impaired myocardial fatty acid metabolism in dialysis patients with normal coronary arteries. Kidney Int. 2006; 69:553–9. [PubMed: 16395255]
77. Fink JC, Lodge MA, Smith MF, et al. Pre-clinical myocardial metabolic alterations in chronic kidney disease. Cardiology. 2010; 116:160–7. [PubMed: 20606430]
78. Nishimura M, Tsukamoto K, Hasebe N, Tamaki N, Kikuchi K, Ono T. Prediction of cardiac death in hemodialysis patients by myocardial fatty acid imaging. J Am Coll Cardiol. 2008; 51:139–45. [PubMed: 18191738]
79. Paternostro G, Camici PG, Lammertsma AA, et al. Cardiac and skeletal muscle insulin resistance in patients with coronary heart disease. A study with positron emission tomography. J Clin Invest. 1996; 98:2094–9. [PubMed: 8903329]
80. Mäki M, Luotolahti M, Nuutila P, et al. Glucose uptake in the chronically dysfunctional but viable myocardium. Circulation. 1996; 93:1658–66. [PubMed: 8653871]
81. Pauly DF, Pepine CJ. The role of carnitine in myocardial dysfunction. Am J Kidney Dis. 2003; 41:S35–43. [PubMed: 12751052]
82. Sakurabayashi T, Takaesu Y, Haginoshita S, et al. Improvement of myocardial fatty acid metabolism through l-carnitine administration to chronic hemodialysis patients. Am J Nephrol. 1999; 19:480–4. [PubMed: 10460938]
83. Fujibayashi Y, Yonekura Y, Tamaki K. Myocardial accumulation of BMIPP in relation to ATP concentration. Ann Nucl Med. 1993; 7(suppl 2):15–8.
84. Wishart DS, Knox C, Guo AC, et al. Hmdb: A knowledgebase for the human metabolome. Nucleic Acids Res. 2009; 37:D603–10. [PubMed: 18953024]
85. Bain JR, Stevens RD, Wenner BR, Ilkayeva O, Muoio DM, Newgard CB. Metabolomics applied to diabetes research: Moving from information to knowledge. Diabetes. 2009; 58:2429–43. [PubMed: 19875619]
86. Shah SH, Bain JR, Muehlbauer MJ, et al. Association of a peripheral blood metabolic profile with coronary artery disease and risk of subsequent cardiovascular events. Circ Cardiovasc Genet. 2010; 3:207–14. [PubMed: 20173117]
87. Segers VF, Lee RT. Stem-cell therapy for cardiac disease. Nature. 2008; 451:937–42. [PubMed: 18288183]
88. Lau JF, Anderson SA, Adler E, Frank JA. Imaging approaches for the study of cell-based cardiac therapies. Nat Rev Cardiol. 2010; 7:97–105. [PubMed: 20027188]
89. Hofmann M, Wollert KC, Meyer GP, et al. Monitoring of bone marrow cell homing into the infarcted human myocardium. Circulation. 2005; 111:2198–202. [PubMed: 15851598]
90. Lee AS, Xu D, Plews JR, et al. Preclinical derivation and imaging of autologously transplanted canine induced pluripotent stem cells. J Biol Chem. 2011; 286:32697–704. [PubMed: 21719696]
91. Simioniuc A, Campan M, Lionetti V, et al. Placental stem cells pre-treated with a hyaluronan mixed ester of butyric and retinoic acid to cure infarcted pig hearts: A multimodal study. Cardiovasc Res. 2011; 90:546–56. [PubMed: 21257613]

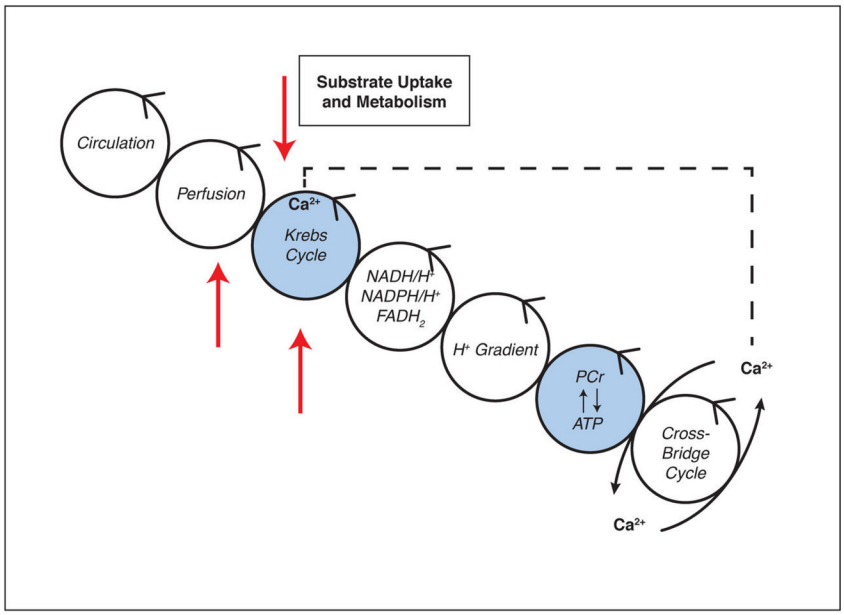


**Figure 1. Energy is transferred along a series of conserved cycles, starting at coronary circulation and ending at cross-bridge formation of contractile elements**

Calcium release from the sarcoplasmic reticulum triggers calcium uptake into the mitochondria and activation of dehydrogenases in the Krebs cycle. Radiolabeled tracers in combination with SPECT or PET (red arrows) and NMR spectroscopy (blue cycles) can assess various cycles noninvasively in vivo. NAD(P)H/$H^+$: reduced nicotinamide adenine dinucleotide (phosphate); FADH2: reduced flavin adenine dinucleotide; PCr: phosphocreatine.

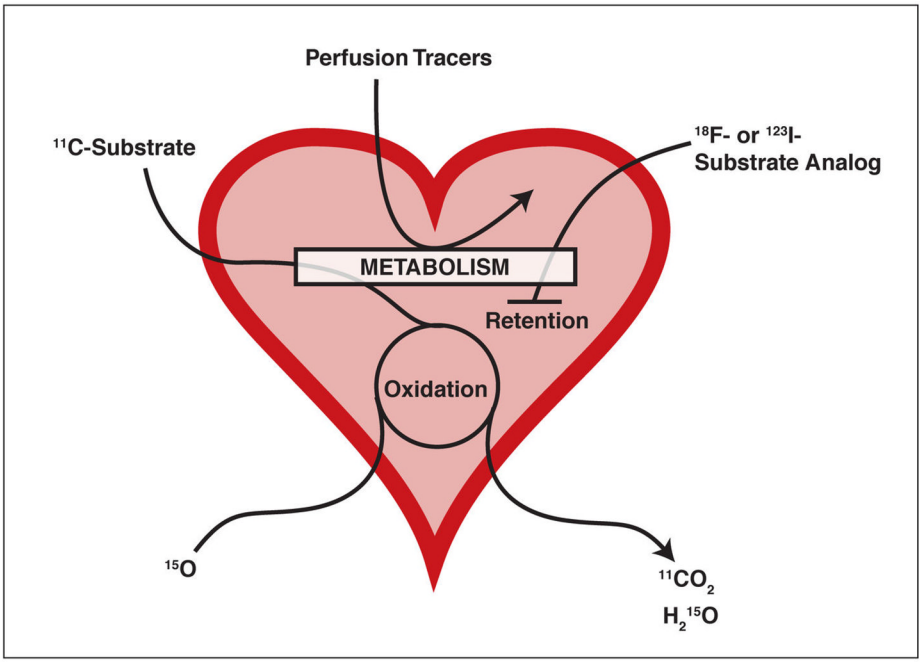


**Figure 2. Schematic overview of the fate of labeled substrates and substrate analogs**

Radiolabeled $^{11}$C-substrate is taken up into the cell and undergoes complete oxidation, eventually leading to the release of $^{11}$CO2. After their uptake into the cell, substrate analogs labeled with $^{18}$F or $^{123}$I are partially metabolized and then retained. The majority of perfusion tracers require preserved cellular metabolism to be taken up by the cell. Substrate oxidation rates can also be monitored using $^{15}$O and measuring the release of H2$^{15}$O.

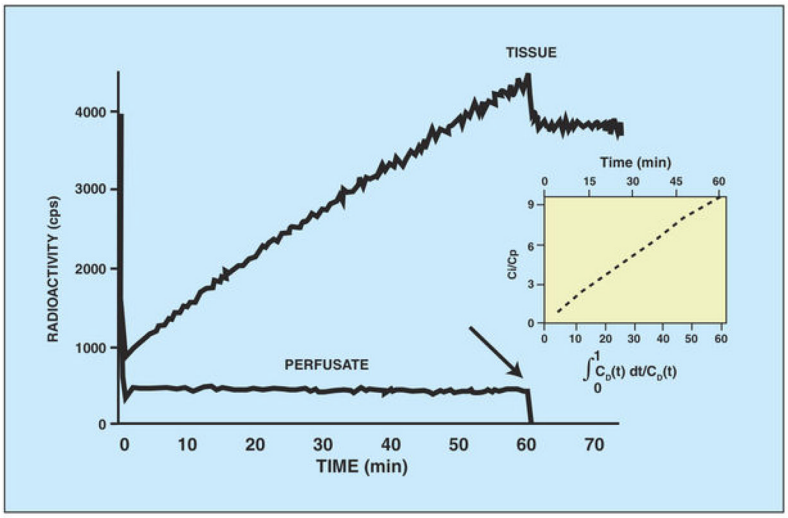


**Figure 3. Diagram showing linear increase of radioactivity in the heart during perfusion with $^{18}$F-fluorodeoxyglucose-containing buffer**

Note that tissue radioactivity remains constant after a tracer-free buffer was used (arrow). Cardiac power was unchanged throughout the experiment (not shown). Patlak analysis shows linear tracer uptake with time (insert).

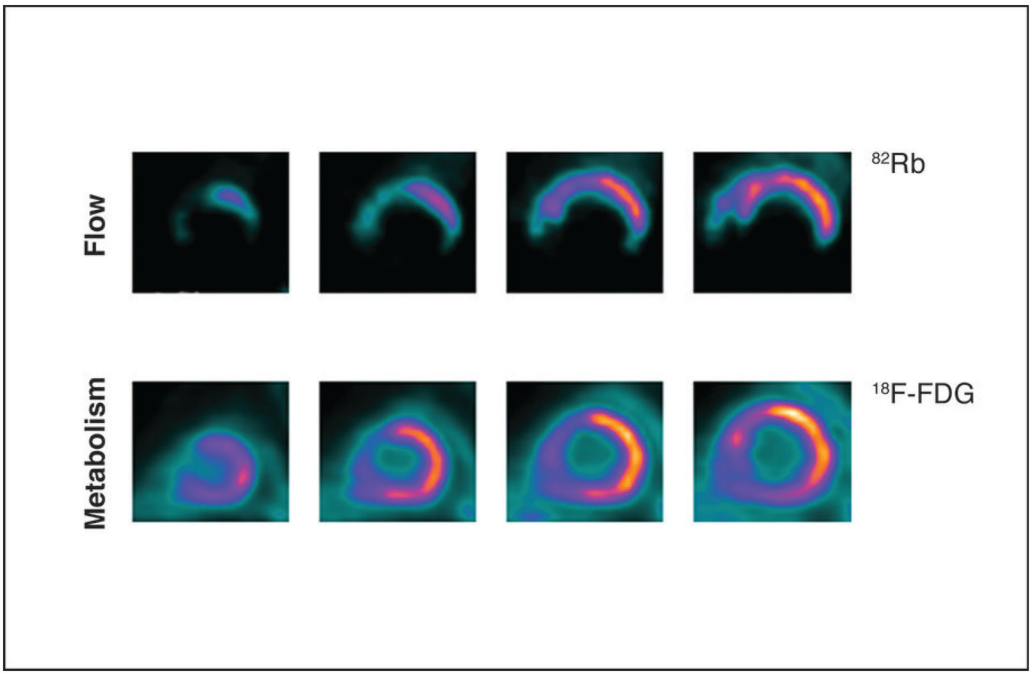


**Figure 4. PET scan showing hibernating myocardium, revealing perfusion-metabolism mismatch**

(**UPPER COLUMN**) Blood flow imaging using rubidium 82 in short-axis view shows markedly decreased perfusion, extending from distal to basal slices in the apical, inferior, inferolateral and septal regions of the left ventricle at rest. (**LOWER COLUMN**) [$^{18}$F]-fluorodeoxyglucose-labeled PET images acquired under glucose-loaded conditions shows preserved glucose utilization in abnormally perfused myocardium, except for the anteroseptal region, in which a metabolism matches perfusion. $^{18}$F-FDG: $^{18}$Ffluorodeoxyglucose; $^{82}$Rb: rubidium 82. (58)

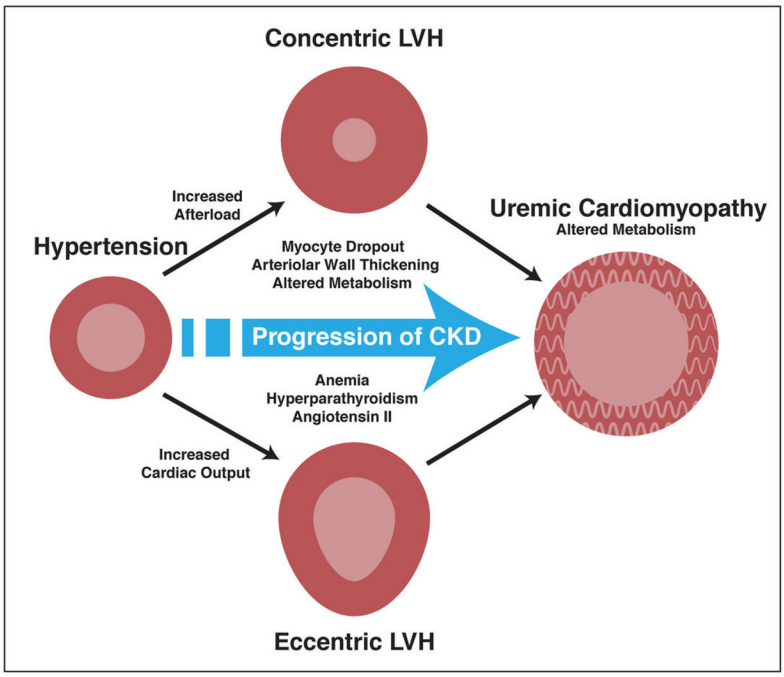


**Figure 5. Pathogenic factors contributing to the development of uremic cardiomyopathy in the setting of chronic kidney disease**

See text for further discussion. LVH: left ventricular hypertrophy; CKD: chronic kidney disease (*with permission from JACC* ref. 70)

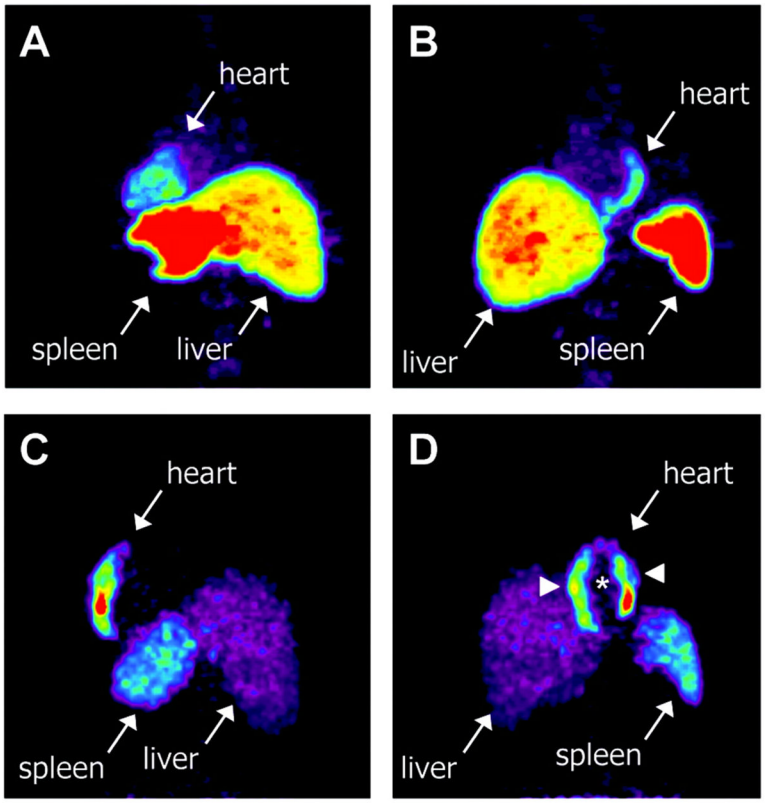


**Figure 6. Myocardial homing and biodistribution of $^{18}$F-FDG–labeled BMCs**

Left posterior oblique (**A**) and left anterior oblique (**B**) views of chest and upper abdomen of patient 2 taken 65 minutes after transfer of $^{18}$F-FDG–labeled, unselected BMCs into left circumflex coronary artery. BMC homing is detectable in the lateral wall of the heart (infarct center and border zone), liver, and spleen. Left posterior oblique (**C**) and left anterior oblique (**D**) views of chest and upper abdomen of patient 7 taken 70 minutes after transfer of $^{18}$F-FDG–labeled, CD34-enriched BMCs into left anterior descending coronary artery. Homing of CD34enriched cells is detectable in the anteroseptal wall of the heart, liver, and spleen. CD34$^{+}$ cell homing is most prominent in infarct border zone (arrowheads) but not infarct center (asterisk) (*with permission from Circulation* – ref. 89).